

# Microstructure and microwave dielectric properties of low-temperature sinterable $(1 - x)\text{Ba}_3(\text{VO}_4)_2-x\text{CaWO}_4$ composite ceramics

Yang Lv · Ruzhong Zuo

Received: 14 August 2012 / Accepted: 8 September 2012 / Published online: 15 September 2012  
© Springer Science+Business Media, LLC 2012

**Abstract** Low-temperature-sintered  $\text{Ba}_3(\text{VO}_4)_2\text{-CaWO}_4$  composite ceramics were prepared by cofiring mixtures of pure-phase  $\text{Ba}_3(\text{VO}_4)_2$  and  $\text{CaWO}_4$ . The thermo-mechanical analysis revealed that the  $\text{CaWO}_4$  in the composite ceramic can significantly promote the densification process and lower the sintering temperature to  $\sim 900^\circ\text{C}$ . The X-ray diffraction results indicated that  $\text{Ba}_3(\text{VO}_4)_2$  and  $\text{CaWO}_4$  phases coexist in the sintered ceramics, and no secondary phases can be detected in the composite, implying the good chemical compatibility between the two phases. The near-zero temperature coefficients of the resonant frequency ( $\tau_f$ ) could be achieved by adjusting the relative content of the two phases owing to their opposite  $\tau_f$  values. The composite ceramics with 60 wt%  $\text{CaWO}_4$  sintered at  $900^\circ\text{C}$  exhibited desirable microwave dielectric properties of the quality factor  $Q \times f \sim 37,000$  GHz, dielectric constant  $\varepsilon_r \sim 12$ , and  $\tau_f \sim -1.4$  ppm/ $^\circ\text{C}$ .

## 1 Introduction

The rapid development of modern wireless communication technologies, such as cellular phones and the global positioning system, has brought a widespread attention to the high-performance microwave dielectric ceramics. To meet the requirement of microwave devices such as multilayer integrated circuits (MIC), wireless LAN, and intelligent transport systems [1–3], microwave dielectric ceramics with a low dielectric constant ( $\varepsilon_r$ ), a high quality factor

( $Q \times f$ ), and a near-zero temperature coefficient of resonant frequency ( $\tau_f$ ) are strongly required. Moreover, the development of low-temperature cofired ceramic (LTCC) has been stimulated by the benefits from the fabrication of miniature multilayer devices [4]. For LTCC applications, the sintering temperature of dielectric ceramics must be lower than the melting points of the electrode metals, for example,  $961^\circ\text{C}$  for silver or  $1,064^\circ\text{C}$  for copper [4]. Therefore, the low temperature sintering is a critical requirement for commercial LTCC applications.

$\text{CaWO}_4$  has been investigated as a potential microwave dielectric ceramic since it exhibits a low  $\varepsilon_r$  ( $\sim 10$ ) and a high  $Q \times f$  value ( $\sim 75,000$  GHz) [5]. However, its large negative  $\tau_f$  values ( $-25$  ppm/ $^\circ\text{C}$ ) and relatively high sintering temperature ( $1,100^\circ\text{C}$ ) limited its application in LTCC devices. A lot of work has been done to decrease its sintering temperature below  $950^\circ\text{C}$  [5, 6]. Although its high sintering temperature can be effectively decreased, its large negative  $\tau_f$  values also need to be compensated.

In order to achieve a microwave dielectric material with a near-zero  $\tau_f$  value, the most effective way is to add a material with an opposite  $\tau_f$  value to compose a composite ceramic. A near-zero  $\tau_f$  value can be easily obtained by altering the relative contents of two phases. The  $0.74\text{CaWO}_4\text{-}0.26\text{TiO}_2$  (volume fraction) composite ceramic sintered at  $1,200^\circ\text{C}$ , exhibits a  $\tau_f$  value  $\sim 0$  ppm/ $^\circ\text{C}$ , a  $\varepsilon_r$  value of 17, and a deteriorated  $Q \times f$  value of 27,000 GHz [7].  $\text{TiO}_2$  has a high sintering temperature of  $1,500^\circ\text{C}$ , which tends to degrade the sinterability and microwave dielectric properties of the composite.

Compared with  $\text{TiO}_2$  and  $\text{CaTiO}_3$  with positive  $\tau_f$  values,  $\text{Ba}_3(\text{VO}_4)_2$  can be sintered at a relatively low temperature ( $1,100^\circ\text{C}$ ) and has a large positive  $\tau_f$  value ( $+52$  ppm/ $^\circ\text{C}$ ) and good microwave dielectric properties ( $\varepsilon_r \sim 14$  and  $Q \times f \sim 42,000$  GHz) [8]. As a result, it is

Y. Lv · R. Zuo (✉)  
Institute of Electro Ceramics and Devices, School of Materials Science and Engineering, Hefei University of Technology, Hefei 230009, People's Republic of China  
e-mail: piezolab@hfut.edu.cn

often used as a  $\tau_f$ -tailoring material to construct composite ceramics, such as  $\text{Ba}_3(\text{VO}_4)_2\text{-Mg}_2\text{SiO}_4$  and  $\text{Ba}_3(\text{VO}_4)_2\text{-BaWO}_4$ , etc. [9, 10]. In these composite ceramics, different crystal structures between two phases have effectively restricted the formation of the solid solutions and the appearance of the secondary phases, and guaranteed the ideal microwave dielectric properties simultaneously with near-zero tunable temperature coefficients.

As  $\text{CaWO}_4$  has a large negative  $\tau_f$  value, one can expect that a dielectric composite material with a near-zero  $\tau_f$  value and a high  $Q \times f$  value could be obtained by incorporating  $\text{CaWO}_4$  and  $\text{Ba}_3(\text{VO}_4)_2$ . In this work, both phase-pure  $\text{Ba}_3(\text{VO}_4)_2$  and  $\text{CaWO}_4$  were separately synthesized by a conventional mixed oxide route.  $(1-x)\text{Ba}_3(\text{VO}_4)_2\text{-}x\text{CaWO}_4$  composite ceramics have been manufactured for the first time and their microwave dielectric properties were investigated systematically.

## 2 Experimental procedure

Samples with compositions of  $(1-x)\text{Ba}_3(\text{VO}_4)_2\text{-}x\text{CaWO}_4$  ( $x = 0.2\text{--}0.6$ , in weight percent) were prepared by a conventional solid-state reaction technique. The starting materials used were high-purity (>99 %) powders of  $\text{BaCO}_3$ ,  $\text{V}_2\text{O}_5$ ,  $\text{CaCO}_3$ , and  $\text{WO}_3$ . Both of  $\text{Ba}_3(\text{VO}_4)_2$  and  $\text{CaWO}_4$  powders were prepared using a conventional mixed oxide method by calcining at  $800^\circ\text{C}$  for 4 h. After ball milling for 12 h, the as-synthesized  $\text{Ba}_3(\text{VO}_4)_2$  and  $\text{CaWO}_4$  powders were then mixed together by ball milling with poly vinyl alcohol (PVA) as a binder. The granulated powders were subsequently pressed into cylinders with dimensions of 10 mm in diameter and of 7–8 mm in height. These specimens were first heated at  $550^\circ\text{C}$  in air for 4 h to burn out the organic binder, and then sintered in air in the temperature range of  $850\text{--}1,000^\circ\text{C}$  for 4 h.

The bulk densities of the sintered samples were measured by the Archimedes method. The relative densities of the specimens were obtained from the bulk density and the theoretical densities by using the following equation [11]:

$$\rho = \frac{w_1 + w_2}{w_1/\rho_1 + w_2/\rho_2} \quad (1)$$

where  $\rho_1$  and  $\rho_2$  are the theoretical density of  $\text{Ba}_3(\text{VO}_4)_2$  and  $\text{CaWO}_4$  ( $5.176\text{ g/cm}^3$  for  $\text{Ba}_3(\text{VO}_4)_2$  phase and  $6.10\text{ g/cm}^3$  for  $\text{CaWO}_4$  phase) [10, 12], respectively;  $w_1$  and  $w_2$  are the weight fraction of  $\text{Ba}_3(\text{VO}_4)_2$  and  $\text{CaWO}_4$ , respectively. The crystal structure of the calcined powders and sintered ceramics was examined by an X-ray diffractometer (XRD, D/Max2500 V, Rigaku, Japan) using  $\text{CuK}\alpha$  radiation. The shrinkage curves were measured using thermal mechanical analysis (TMA, Model 409PC, Netzsch, Selb, FRG). The grain morphology and compositions

were analyzed by a scanning electron microscope (SEM, SSX-550, Shimadzu, Japan) equipped with an energy dispersive spectrometer (EDS). An Agilent N5230C network analyzer (Agilent, Santa Clara, CA, USA) was used for the measurement of microwave dielectric properties by means of a Hakki-Coleman method [13, 14]. The  $\tau_f$  value of the samples was measured in the temperature range from  $30$  to  $80^\circ\text{C}$ . It can be calculated by the following relationship:  $\tau_f = \frac{f_2 - f_1}{f_1(T_2 - T_1)}$ , where  $f_1$  and  $f_2$  represent the resonant frequencies at  $T_1$  and  $T_2$ , respectively.

## 3 Results and discussion

Figure 1 shows the XRD patterns of  $(1-x)\text{Ba}_3(\text{VO}_4)_2\text{-}x\text{CaWO}_4$  composite ceramics sintered at  $900^\circ\text{C}$  for 4 h. All the main peaks can be indexed in terms of  $\text{Ba}_3(\text{VO}_4)_2$  (JCPDS #29-0211) and  $\text{CaWO}_4$  (JCPDS #41-1431), and there is no trace of any secondary phases. This suggests that the composite ceramic has been formed and no obvious reaction has occurred. The crystal structure of  $\text{Ba}_3(\text{VO}_4)_2$  is hexagonal R32/m, with the  $\text{V}^{5+}$  ions located in the center of tetrahedral  $[\text{VO}_4]$  units linked by sixfold and tenfold coordinate  $\text{Ba}^{2+}$  ions [15]. However,  $\text{CaWO}_4$  has a tetragonal symmetry and the coordination number of the  $\text{Ca}^{2+}$  ions is eight while the coordination number of the  $\text{W}^{6+}$  ions is four [16]. The big difference in the crystal structures and the good stability of both phases significantly limits the formation of solid solutions between  $\text{Ba}_3(\text{VO}_4)_2$  and  $\text{CaWO}_4$ .

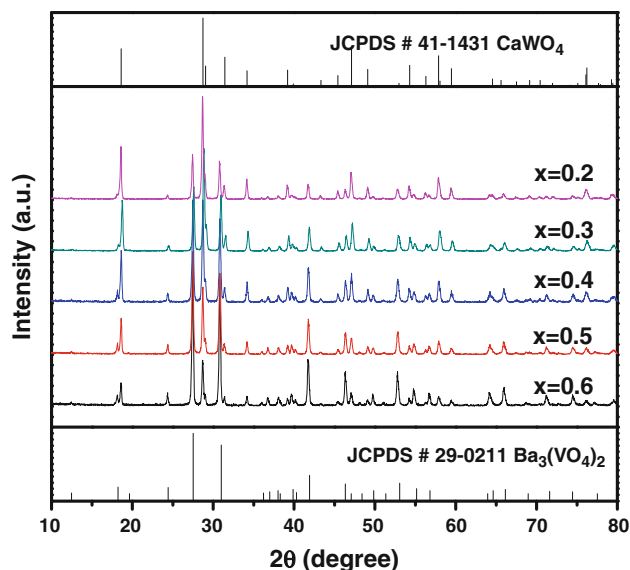


**Fig. 1** XRD patterns of  $(1-x)\text{Ba}_3(\text{VO}_4)_2\text{-}x\text{CaWO}_4$  ( $x = 0.2\text{--}0.6$ ) ceramics sintered at  $900^\circ\text{C}$  for 4 h, as compared to the standard patterns of  $\text{Ba}_3(\text{VO}_4)_2$  and  $\text{CaWO}_4$

**Fig. 2** SEM images of the  $(1-x)\text{Ba}_3(\text{VO}_4)_2-x\text{CaWO}_4$  ceramics: **a**  $x = 0.2$ , at  $900^\circ\text{C}$ , **b**  $x = 0.3$ , at  $900^\circ\text{C}$ , **c**  $x = 0.4$ , at  $900^\circ\text{C}$ , **d**  $x = 0.5$ , at  $900^\circ\text{C}$ , **e**  $x = 0.6$ , at  $900^\circ\text{C}$ , **f**  $x = 0.6$  (EDS image), at  $900^\circ\text{C}$ , **g**  $x = 0.6$ , at  $950^\circ\text{C}$ , and **h**  $x = 0.6$ , at  $1,000^\circ\text{C}$

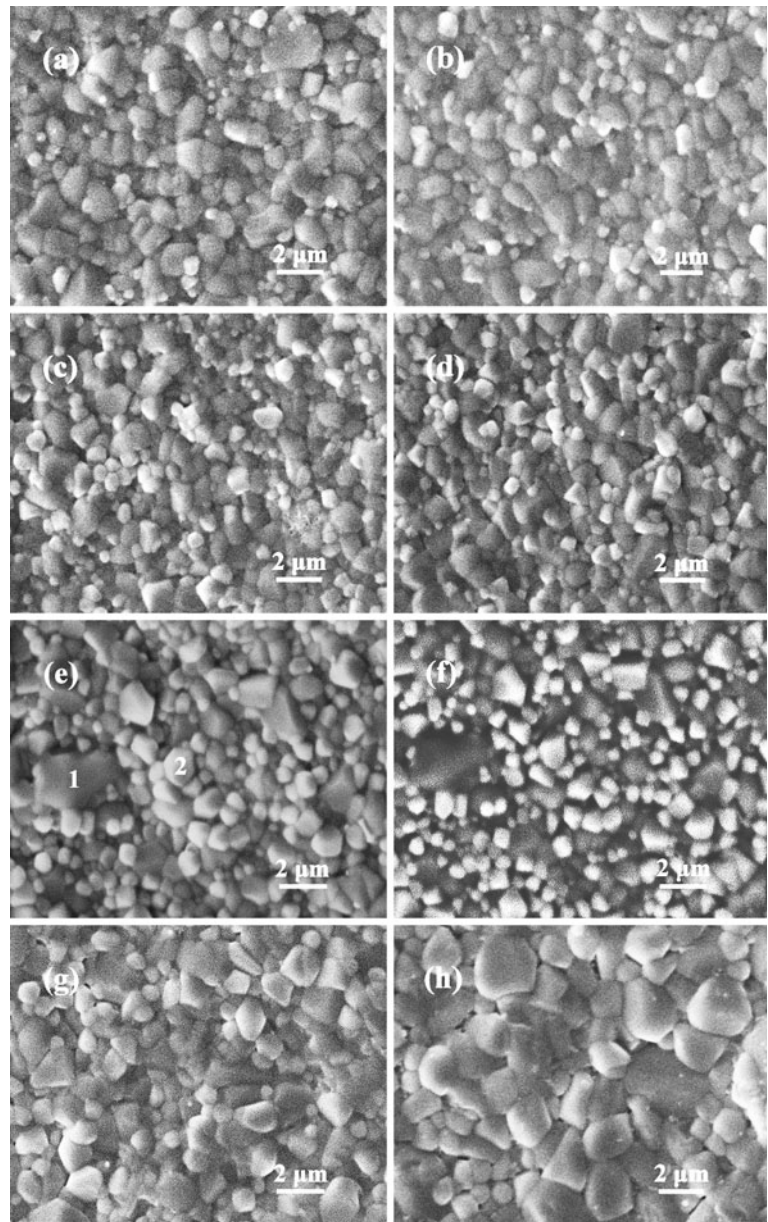


Figure 2 shows the SEM images of  $(1-x)\text{Ba}_3(\text{VO}_4)_2-x\text{CaWO}_4$  ceramics sintered at various temperatures. All samples sintered at  $900^\circ\text{C}$  have a high density without obvious porosity and exhibit an uniform microstructure. In addition, it can be noted that all the specimens exhibit a bimodal grain size distribution. The result of EDS analysis show that big grains (marked 1 in Fig. 2e) mainly contain Ba, V, and O elements in a molar ratio of Ba:V:O = 3:2:8, and that small grains (marked 2 in Fig. 2e) are dominantly composed of Ca, W and O elements in a molar ratio of 1:1:4, as shown in Table 1. The EDS analysis indicates that the big and small grains belong to  $\text{Ba}_3(\text{VO}_4)_2$  and  $\text{CaWO}_4$ , respectively. This kind of two-phase structure can be more straightforwardly observed on a backscattered electron

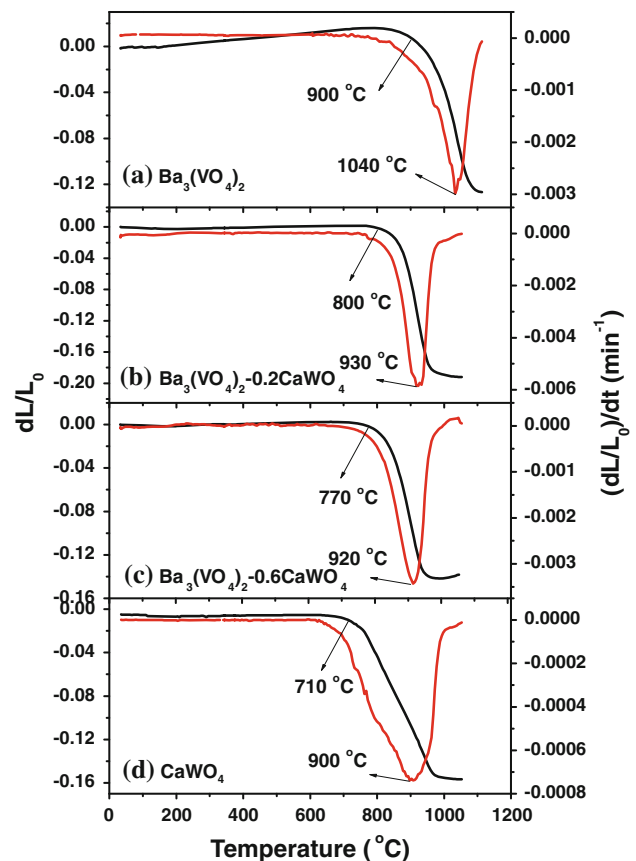
image (Fig. 2f). Because of the different relative atomic mass of W and V, the light-colored grains are rich in W and the dark ones are rich in V. From the EDS results, it also can be seen that a slight ionic diffusion exists in the composite, such as some  $\text{Ca}^{2+}$  and  $\text{W}^{6+}$  ions were detected in the grain of  $\text{Ba}_3(\text{VO}_4)_2$ . Figure 2e, g, h show the grain morphology of  $0.4\text{Ba}_3(\text{VO}_4)_2-0.6\text{CaWO}_4$  samples sintered at  $900$ ,  $950$ , and  $1,000^\circ\text{C}$ , respectively. It can be observed that the grain size and density of the composite increase obviously with increasing the sintering temperature. However, the rapid grain growth tends to lower the sintering driving force for densification, leading to a reduction of the density, as the sintering temperature is too high [9].

**Table 1** EDS analysis of  $0.4\text{Ba}_3(\text{VO}_4)_2\text{-}0.6\text{CaWO}_4$  ceramics sintered at  $900\text{ }^\circ\text{C}$  for 4 h

Elements	Atom %	
	Point 1	Point 2
Ba	25.72	0.00
V	16.30	0.00
O	51.09	68.70
Ca	2.82	15.44
W	4.07	15.86
Total	100.00	100.00

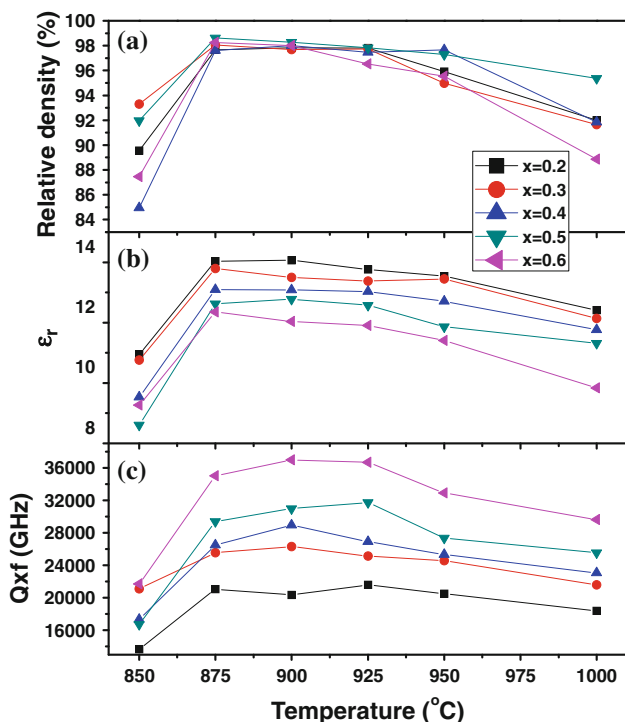
The linear shrinkage behavior and the shrinkage rate as a function of temperature for  $(1-x)\text{Ba}_3(\text{VO}_4)_2\text{-}x\text{CaWO}_4$  samples are shown in Fig. 3. It can be seen that the temperature for the maximum densification rate of  $(1-x)\text{Ba}_3(\text{VO}_4)_2\text{-}x\text{CaWO}_4$  ceramics was slightly lowered with increasing the  $\text{CaWO}_4$  content, probably owing to a lower densification temperature of  $\text{CaWO}_4$  than that of  $\text{Ba}_3(\text{VO}_4)_2$ . Moreover, as the diffusion of  $\text{W}^{6+}$  and  $\text{Ca}^{2+}$  ions into the lattice of  $\text{Ba}_3(\text{VO}_4)_2$  would not only cause a slight lattice distortion of the  $\text{Ba}_3(\text{VO}_4)_2$  phase, but also generate a tiny amount of oxygen vacancies. These lattice defects would also accelerate the mass mobility and make the densification of the composite ceramics occur at a lower temperature.

Figure 4 shows the relative densities,  $\epsilon_r$  and  $Q \times f$  values of  $(1-x)\text{Ba}_3(\text{VO}_4)_2\text{-}x\text{CaWO}_4$  ( $x = 0.2\text{--}0.6$ ) ceramics as a function of the sintering temperature. It can be seen that the sample densities first increase with the sintering temperature and then decrease after a maximum value is reached. It should be noted that the maximum density of approximately 98 % was obtained in the temperature range of  $875\text{--}925\text{ }^\circ\text{C}$  for almost all composite samples. Such a high sample density obtained at a relatively low temperature can be also reflected by the SEM images (Fig. 2). At a lower temperature range, the sintering of the composite ceramics was obviously improved by the increasing the amount of  $\text{CaWO}_4$ . This effect was weakened as the sintering temperature is higher than  $875\text{ }^\circ\text{C}$ , since it gets close to the maximum shrinkage rate of pure  $\text{CaWO}_4$  phase (Fig. 3d). The microwave dielectric properties of  $(1-x)\text{Ba}_3(\text{VO}_4)_2\text{-}x\text{CaWO}_4$  ceramics are shown in Fig. 4(b, c). The dielectric constant  $\epsilon_r$  of the ceramics also initially increases with the sintering temperature and then begins to decrease, which was similar to the trend of the relative densities against the temperature of the ceramics. The  $\epsilon_r$  value of the composite ceramics at the same sintering temperature was found to decrease with increasing the content of  $\text{CaWO}_4$ . It also can be found that the dielectric constant of the  $(1-x)\text{Ba}_3(\text{VO}_4)_2\text{-}x\text{CaWO}_4$  composite ceramics is approximately in between those of

**Fig. 3** Shrinkage and shrinkage rate of  $(1-x)\text{Ba}_3(\text{VO}_4)_2\text{-}x\text{CaWO}_4$  composite samples as a function of temperature

single-phase  $\text{Ba}_3(\text{VO}_4)_2$  and  $\text{CaWO}_4$  ceramics [7, 8]. This is basically ascribed to the mixing rule of dielectrics as expressed by the Maxwell–Wagner’s equation [17]. The  $Q \times f$  values of  $(1-x)\text{Ba}_3(\text{VO}_4)_2\text{-}x\text{CaWO}_4$  composite ceramics also increase with increasing the sintering temperature. For all compositions, the maximum  $Q \times f$  values can be obtained as the sintering temperature is  $900\text{ }^\circ\text{C}$ , then begin to decline by further increasing the sintering temperatures up to  $1,000\text{ }^\circ\text{C}$ . The  $Q \times f$  values of all compositions roughly range from 21,600 to 37,000 GHz, which were lower than those of pure-phase  $\text{Ba}_3(\text{VO}_4)_2$  ( $Q \times f = 42,000\text{ GHz}$ ) and  $\text{CaWO}_4$  ( $Q \times f = 75,000\text{ GHz}$ ) ceramics [6, 7]. This result might be attributed to the doping effect that a slight amount of element such as  $\text{Ca}^{2+}$  and  $\text{W}^{6+}$  ions diffuses into the lattice of  $\text{Ba}_3(\text{VO}_4)_2$  phase during cofiring of  $\text{Ba}_3(\text{VO}_4)_2$  and  $\text{CaWO}_4$  (see Table 1) [18].

The  $\tau_f$  values of  $(1-x)\text{Ba}_3(\text{VO}_4)_2\text{-}x\text{CaWO}_4$  ceramics sintered at various temperatures are shown in Fig. 5. On the one hand, the  $\tau_f$  value of  $\text{Ba}_3(\text{VO}_4)_2$  ceramics obviously varies with changing the sintering temperature as we compare our current data with the reported values [8]. On the other hand, due to the opposite-sign  $\tau_f$  values of



**Fig. 4** Relative density (a) and microwave dielectric properties (b, c) of the  $(1 - x)\text{Ba}_3(\text{VO}_4)_2 - x\text{CaWO}_4$  ceramics as a function of sintering temperature

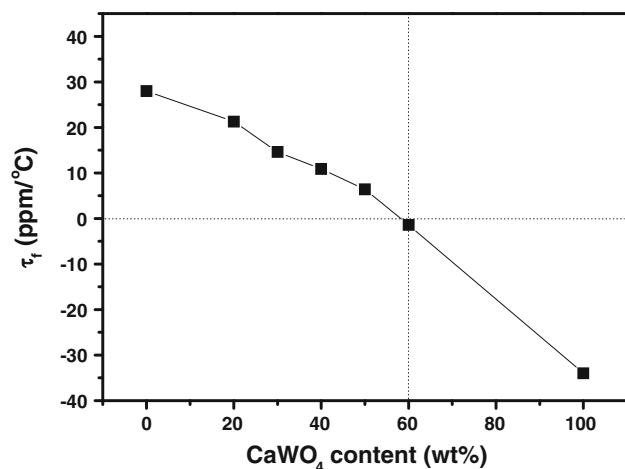


**Fig. 5** The  $\tau_f$  values of the  $(1 - x)\text{Ba}_3(\text{VO}_4)_2 - x\text{CaWO}_4$  ceramics sintered at various temperatures for 4 h:  $x = 0$ , at 1,300 °C;  $x = 0.2 - 0.6$ , at 900 °C and  $x = 1$ , at 1,100 °C

$\text{Ba}_3(\text{VO}_4)_2$  and  $\text{CaWO}_4$ , the  $\tau_f$  values of the composite ceramics decrease with increasing the content of  $\text{CaWO}_4$ . The result indicates that the composite processing should be an effective way to tune the  $\tau_f$  value as required. As a result, the  $0.4\text{Ba}_3(\text{VO}_4)_2 - 0.6\text{CaWO}_4$  composite ceramics sintered at 900 °C exhibit a near-zero  $\tau_f$  value ( $-1.4 \text{ ppm}/^\circ\text{C}$ ), together with an optimum  $Q \times f$  value of 37,000 GHz

and a low  $\epsilon_r$  value of 12. This result demonstrates that  $(1 - x)\text{Ba}_3(\text{VO}_4)_2 - x\text{CaWO}_4$  composite ceramic could be a good low-permittivity LTCC microwave dielectric material as the  $\text{CaWO}_4$  content is appropriately adjusted.

### 4 Conclusions

The low-temperature firable  $(1 - x)\text{Ba}_3(\text{VO}_4)_2 - x\text{CaWO}_4$  microwave dielectric composite ceramics were investigated in this study. The phase structure, grain morphology, sintering behavior, and various microwave dielectric properties were explored as a function of the sintering temperature and the  $\text{CaWO}_4$  content. The XRD results show that a desirable composite ceramic can be obtained, with no indication of any secondary phases after sintering. The thermomechanical analysis and the density measurement demonstrate a low-temperature sinterability of this composite system. During cofiring of two phases, a slight of  $\text{Ca}^{2+}$  and  $\text{W}^{6+}$  diffusion into the  $\text{Ba}_3(\text{VO}_4)_2$  lattice might degrade the  $Q \times f$  values of the composite ceramics. The composite ceramic with 60 wt%  $\text{CaWO}_4$  sintered at 900 °C exhibit desirable microwave dielectric properties of  $\epsilon_r \sim 12$ ,  $Q \times f \sim 37,000 \text{ GHz}$ , and  $\tau_f \sim -1.4 \text{ ppm}/^\circ\text{C}$ .

**Acknowledgments** This work was financially supported by a project of Natural Science Foundation of Anhui Province (1108085J14) and the National Natural Science Foundation of China (50972035 and 51272060).

### References

1. M.T. Sebastian, H. Jantunen, *Int. Mater. Rev.* **53**, 57 (2008)
2. W. Lei, W.Z. Lu, D. Liu, J.H. Zhu, *J. Am. Ceram. Soc.* **92**, 105 (2009)
3. K.P. Surendran, P.V. Bijumon, P. Mohanan, M.T. Sebastian, *Appl. Phys. A* **81**, 823 (2005)
4. M. Guo, S.P. Gong, G. Dou, D.X. Zhou, *J. Alloy Compd.* **509**, 5988 (2011)
5. E.S. Kim, S.H. Kim, B.I. Lee, *J. Eur. Ceram. Soc.* **26**, 2101 (2006)
6. L. Wang, J.J. Bian, *Mater. Lett.* **65**, 726 (2011)
7. S.H. Yoon, G.K. Choi, D.W. Kim, S.Y. Cho, K.S. Hong, *J. Eur. Ceram. Soc.* **27**, 3087 (2007)
8. R. Umemura, H. Ogawa, A. Yokoi, H. Ohsato, A. Kan, *J. Alloy Compd.* **424**, 388 (2006)
9. S.Q. Meng, Z.X. Yue, H. Zhuang, F. Zhao, L.T. Li, *J. Am. Ceram. Soc.* **93**, 359 (2010)
10. H. Zhuang, Z.X. Yue, S.Q. Meng, F. Zhao, L.T. Li, *J. Am. Ceram. Soc.* **91**, 3738 (2008)
11. H. Zhuang, Z.X. Yue, F. Zhao, L.T. Li, *J. Am. Ceram. Soc.* **91**, 3275 (2008)
12. S.H. Yoon, D.W. Kim, S.Y. Cho, K.S. Hong, *J. Eur. Ceram. Soc.* **26**, 2051 (2006)
13. B.W. Hakki, P.D. Coleman, *IEEE Trans. Microwave Theory Technol.* **8**, 402 (1960)
14. W.E. Courtney, *IEEE Trans. Microwave Theory Technol.* **18**, 476 (1970)

15. M.H. Whitmore, H.R. Verdun, D.J. Singel, *Phys. Rev. B.* **47**, 11479 (1993)
16. M.M. Krzmanc, M. Logar, B. Budic, D. Suvorov, *J. Am. Ceram. Soc.* **94**, 2464 (2011)
17. Y.G. Wu, X.H. Zhao, F. Li, Z.G. Fan, *J. Electroceram.* **11**, 227 (2003)
18. S.F. Wang, Y.F. Hsu, Y.R. Wang, C.C. Sung, *J. Am. Ceram. Soc.* **94**, 812 (2011)